



Contents lists available at ScienceDirect

Probabilistic Engineering Mechanics

journal homepage: www.elsevier.com/locate/probengmech

Finite element method based Monte Carlo filters for structural system identification

H.A. Nasrellah¹, C.S. Manohar^{*}

Department of Civil Engineering, Indian Institute of Science, Bangalore 560 012, India

ARTICLE INFO

Article history:

Received 5 October 2009

Received in revised form

17 August 2010

Accepted 17 August 2010

Available online xxxx

Keywords:

Structural system identification

Particle filters

Dynamic state estimation

Bootstrap filter

ABSTRACT

The paper proposes a strategy for combining two powerful computational procedures, namely, the finite element method (FEM) for structural analysis and particle filtering for dynamic state estimation, to tackle the problem of structural system parameter identification based on a set of noisy measurements on static and (or) dynamic structural responses. The proposed identification method automatically inherits the wide ranging capabilities of both FEM and particle filtering procedures thereby enabling the treatment of many complicated features of system identification problems, namely, imperfections in mathematical models for structural behavior, noisy and spatially incomplete measurements, nonlinear models for process and measurement equations, possible non-Gaussian nature of system and measurement noises, and dynamic and (or) static behaviors of the structure. Additionally, the authors propose a method that permits assimilation of measurements from multiple static and (or) dynamic tests and from multiple sensors in the system identification procedure in a unified manner. The paper describes how finite element models residing in commercially available softwares can be made to communicate with a database of measurements via a particle filtering algorithm developed on the Matlab platform. This leads to a probabilistic description of system parameters to be identified. Illustrative examples consider measurements from computational models, laboratory and field tests. These illustrations include studies on a rubber sheet with a hole undergoing large deformations, laboratory investigations on a single span beam and field investigations on an existing multi-span masonry arch bridge subjected to diagnostic moving loads.

© 2010 Elsevier Ltd. All rights reserved.

1. Introduction

The problem of structural system identification constitutes an important and difficult class of inverse problems in structural mechanics. Various methods for identification of parameters of dynamical systems exist and the works of Juang [1], Ljung [2], Maia and De Silva [3], Heylen et al. [4], Bendat [5], Ewins [6], Pintelon and Schoukens [7], Peeters and Roeck [8], Lieven and Ewins [9], Worden and Tomlinson [10], Nelles [11] and Kerschen et al. [12] provide extensive overviews of the state of the art. Several issues related to non-uniqueness of solutions, spatio-temporal incompleteness of response measurements, presence of measurement noise, modeling uncertainties, possible presence of structural nonlinearities, and difficulties arising out of complete/partial lack of measurement of inputs have been addressed in these studies. The related problems of finite element model updating and vibration

based structural damage detection have also received wide attention [13–15]. The focus of the present study is on exploring the application of identification methods that are based on dynamic state estimation (DSE) techniques. Specifically, we aim to develop identification procedures that account for following problem features: (a) structural modeling using the finite element (FE) method (especially when these models reside in commercially available FE analysis packages), (b) availability of a set of (noisy, spatially incomplete, static/dynamic) measurement data on strains, displacements and (or) accelerations, and (c) possibility of the structure behaving nonlinearly.

The problem of DSE is typically stated in the discrete state space form and consists of determination of conditional probability density function (pdf) of system states given a set of measurements. The errors in formulating the mathematical models governing the system states and measurements and also the sensor noises in acquiring measurements are treated as a sequence of identical independent random vectors. Consequently the vector of system states is modeled as a Markov vector and the application of Bayes' theorem leads to a set of recursive relations for evolution of the posterior pdf conditioned on available measurements [16]. These relations are formulated in

^{*} Corresponding author. Tel.: +91 80 2293 3121; fax: +91 80 2360 0404.

E-mail address: manohar@civil.iisc.ernet.in (C.S. Manohar).

¹ Doctoral student; also, Lecturer, Alzaiem Alazhari University, Khartoum, Sudan.

terms of a set of multi-dimensional integrals which, most often, are not amenable for closed-form solutions nor can they be practically be evaluated using rules of numerical quadrature. For linear state space models with additive Gaussian noises, an exact solution to this problem was developed by Kalman [17] and this formulation forms the cornerstone of many practical engineering applications [18–21]. For nonlinear processes and (or) measurement equations with additive Gaussian noises, one could linearize the evolving states along a reference trajectory and apply the Kalman filter on the resulting approximate equations and such an algorithm is known as the extended Kalman filter (EKF) [19]. For a more general class of problems involving nonlinear state space models and (or) non-Gaussian additive/multiplicative noises, Monte Carlo simulation strategy could be used to recursively evaluate the multi-dimensional integrals and these methods are styled variously as particle filters, Monte Carlo filters, Bayesian filters or population Monte Carlo algorithms [22–30,16,31,32].

The problem of structural system identification can be brought into the folds of DSE problems and different options are available in the existing literature to achieve this. One option is to declare the vector of system parameters to be identified as additional state variables and augment the original state vector by these artificial state variables. The solution to the resulting state estimation problem also contains the estimates of the posterior pdf-s of the system parameters. It may be noted that, since system parameters often multiply the system states, the problem of DSE here becomes nonlinear in nature even when the original process and measurement equations are linear. Consequently, the DSE problem here could be solved using extended Kalman filtering or particle filtering strategies. The studies by Yun and Shinozuka [33], Hoshiya and Saito [34], Imai et al. [35] are perhaps some of the earliest investigations on the application of the EKF algorithm for identification of parameters of linear and nonlinear structural systems. More recently, the question of identification of parameters of deteriorating structures using EKFs combined with finite element discretization, has been discussed by Corigliano and Mariani [36]. The work of Ghosh et al. [37] describes the development of novel forms of EKFs which are based on derivative-free transversal linearization schemes for handling the nonlinear process equations. The idea of using particle filters to estimate the combined state vector of system states and system parameters is being explored in the area of structural system identification over the last five years [38–42].

The next option to estimate system parameters, within the ambit of DES methods, is to combine maximum likelihood estimation along with state estimation. Here an assumption on joint pdf of the system parameters to be estimated needs to be made and often recourse is made to Gaussian models [43,44]. The study by Namdeo and Manohar [45] offers another alternative for system parameter identification using DSE techniques. Here the parameters of the system, which are to be identified, are treated as a set of random variables with finite number of discrete states. The authors consider nonlinear systems and develop a procedure that combines a bank of self-learning particle filters with a global iteration strategy to estimate the probability distribution of the system parameters to be identified and no *ad hoc* assumption of pdf of parameters to be identified is made.

In the broader context of signal processing and applied statistics, the problem of identification of time invariant parameters of dynamical systems using DSE tools has been widely researched upon (see, for example, the works of Liu and West [46], Storvik [47], Chopin [48], Doucet and Tadic, [49], and Ionides et al. [50]). To the best of present authors' knowledge the ramifications of this body of knowledge in the context of structural system identification has not been explored in the existing literature.

The recent work by the present authors [51,52] consider system identification problem in which measurement data emanate from multiple sensor types and multiple test scenarios. The authors consider situations in which measurements on strains and displacements at a set of points are available from static tests (load–displacement tests and quasi-static moving load tests) and dynamic tests (measurement of frequency response functions (FRF-s) for linear systems). A dummy independent variable which takes values on a unit interval is introduced and the entire set of measurement data from multiple tests and multiple sensors are assimilated into the mathematical model using a pseudo-sequencing approach. Both the Kalman filter (after using a one-term Neumann's expansion on structural stiffness matrix) and particle filtering strategies have been proposed for the purpose of data assimilation. The studies conducted so far have shown promise for further extension to cover dynamical behavior of nonlinear systems and also for extension to study large scale problems. These extensions would be greatly facilitated if the identification procedure readily employs existing FE analysis softwares and avoids the duplication of FE code development while performing system identification. Accordingly, the present study is taken up with the following objectives:

- embedding finite element procedures into the system identification algorithm for time domain analysis of linear/nonlinear dynamical systems,
- combining the particle filtering algorithm with FEM by developing interfaces between FE models residing in readily available commercial codes and DSE algorithms developed on the Matlab platform,
- uncoupling the problems of state estimation and parameter estimation which offers particular advantage in fusing measurement data from multiple tests (and hence assimilation into multiple mathematical models) and in avoiding treatment of a large number of state variables in the DSE problem,
- consider a modification to the filtering algorithm that takes into account the fact that the system parameters being estimated are essentially time invariant in nature and it is desirable to lessen the number of calls to the FE code especially when assimilating large amount of vibration measurement data acquired at high sampling rates, and
- illustration of proposed strategy for problems of SSI when measurement data emanate from computational codes, laboratory experiments and field investigations.

The range of examples covered include a rubber sheet with hole undergoing large amplitude static/dynamic displacements; laboratory studies on a single span beam; and, a multi-span arch railway bridge structure which has been tested for its static behavior. The last example is drawn from ongoing studies being conducted by the present authors and their colleagues on conditional assessment of existing railway bridges in India. This investigation itself is motivated by the long term objective of Indian Railways to increase the axle loads of the freight formations, increase movement speeds and lengths of formations and the concomitant need to ascertain the capabilities of the existing bridge structures to cope up with these enhanced demands.

As has been already noted, the literature in the area of mathematical statistics contains several alternate versions of DSE tools to treat the problem of estimation of static parameters of dynamical models. In the present study we are adopting one of the earlier versions of the particle filtering method with focus of the study being on exploring the parameters of FE structural models based on multiple static and (or) dynamic test data. The overall framework of combining DSE tools and FE models could be retained even if more sophisticated particle filtering tools are used.

Table 1

The artificial independent variable a_i for different types of tests.

No.	Test	Independent variable
1	Incremental load–displacement test in which externally applied loads are incremented as $P_j = \alpha_j P_0, j = 1, 2, \dots, N_1$ where P_0 is a reference value	$a = \alpha$ with $a_l = 1$ and $a_u = N_1$
2	Quasi-static moving load test in which a set of forces move quasi-statically and the position of the leading load from one of the ends of the structure is denoted by β	$a = \beta$ with $a_l = \beta_{\min}$ and $a_u = \beta_{\max}$
3	Measurement of a set of FRF-s of the structure using either the impulse hammer test or the modal shaker test over the frequency range $\omega_{\min} \leq \omega \leq \omega_{\max}$	$a = \omega$ with $a_l = \omega_{\min}$ and $a_u = \omega_{\max}$
4	Measurement of response time histories over the time duration $t_{\min} \leq t \leq t_{\max}$	$a = t$ with $a_l = t_{\min}$ and $a_u = t_{\max}$

2. Combined FEM and DSE techniques for system identification

We consider the structural model with parameters $\theta_i, i = 1, 2, \dots, p$. These parameters could represent structural stiffness, damping, mass properties and parameters associated with the specification of boundary conditions. The structural behavior could be linear or nonlinear and static or dynamic. When considering dynamic behavior, the parameters $\theta_i, i = 1, 2, \dots, p$ are taken to be time-invariant. We consider that a set of N_T different tests have been conducted on the structural system to be identified. These tests could be static and (or) dynamic in nature; for instance, they could include static load–deflection tests, quasi-static moving load tests, measurement of FRF-s using either the impulse hammer test or the modal shaker test, or measurement time histories of response either under measured or unmeasured external dynamic forces. Associated with each of these test scenarios, we introduce independent variables $\{a_i\}_{i=1}^{N_T}$ such that $a_{il} \leq a_i \leq a_{iu}$ and consider the system response in i -th test to evolve in the variable a_i (see Table 1). While for dynamic tests the time variable t is the obvious choice for the independent variable and system response indeed ‘evolves’ in t , for other tests, the notion of an independent variable and evolution along this variable is introduced deliberately to facilitate data assimilation via DSE techniques. When considering measurement data originating from more than one test it is expeditious to introduce a common independent variable τ . Thus, when all the four tests mentioned in Table 1 are performed on a given structure, we take

$$\tau = \frac{\alpha - \alpha_{\min}}{\alpha_{\max} - \alpha_{\min}} = \frac{\beta - \beta_{\min}}{\beta_{\max} - \beta_{\min}} = \frac{\omega - \omega_{\min}}{\omega_{\max} - \omega_{\min}} = \frac{t - t_{\min}}{t_{\max} - t_{\min}}. \quad (1)$$

Clearly, as the variables α, β, ω and t take values over their respective ranges, the variable τ takes values from 0 to 1. The system parameters of interest $\theta_i, i = 1, 2, \dots, p$ are independent of the variables α, β, ω and t and hence independent of τ . Indeed, we postulate that the statements

$$\frac{d\theta_i}{d\tau} = 0; \quad \theta_i(\tau = 0) = \theta_{i0}; \quad i = 1, 2, \dots, p; \quad (2)$$

constitute the set of process equations in the DSE formulation. If the variable τ is discretized such that $\tau_k = \tau/N_T$, and, by using the notation $\theta_{ik} = \theta_i(\tau = \tau_k)$, the above equation can be written as

$$\theta_{ik+1} = \theta_{ik}; \quad i = 1, 2, \dots, p; \quad k = 1, 2, \dots, N_T. \quad (3)$$

Suppose that, for each of the tests mentioned in Table 1, we use a set of N_s sensors, consisting of strain gauges, LVDT-s, accelerometers, tilt meters etc., we could acquire a suite of measurements and we denote this by a $N_y \times 1$ vector $y_k; k = 1, 2, \dots, N_T$. Here the size $N_y \times 1$ of the measurement vector depends upon the number of sensors used and number of tests performed. Clearly, $y_k; k = 1, 2, \dots, N_T$ depends upon the system parameters $\theta_i, i = 1, 2, \dots, p$ and we need to postulate a mathematical model to capture dependence. To achieve this, we postulate that a set of FE models for the structure under study

can be formulated so that each of these models correspond to one testing scenario listed in Table 1. To clarify this further, it may be noted that these models could be linear or nonlinear in nature and could represent static or dynamic behavior of the system. In any case, each of the FE models would have $\theta_i, i = 1, 2, \dots, p$ as the common set of model parameters. In the present study we assume that these FE models reside in professional FE softwares that are commercially available and, in our work, we have utilized the NISA family of finite element softwares. We represent the model for measurements using the equation

$$y_k = h_k(\theta_{1k}, \theta_{2k}, \dots, \theta_{pk}) + \xi_k; \quad k = 1, 2, \dots, N_T. \quad (4)$$

Here $h_k(\theta_k)$ denotes the set of outputs from the suite of FE models with input parameters $\theta_i = \theta_{ik}; i = 1, 2, \dots, p$ and which serve as approximation to the measured quantities $y_k; k = 1, 2, \dots, N_T$. The quantity ξ_k represents a $N_y \times 1$ vector of random variables with a specified probability density function (pdf) given by $p(\xi_k)$. This random quantity models the errors made in relating the measured quantities $y_k; k = 1, 2, \dots, N_T$ with the ‘system states’ $\theta_i, i = 1, 2, \dots, p$ through the postulated FE model and also the effect of measurement noise that is invariably present while measuring system responses. We assume that the random vectors ξ_k for $k = 1, 2, \dots, N_T$ constitute a sequence of identical and independent random variables and this assumption is consistent with assumptions that are commonly made in implementing DSE techniques. The problem on hand consists of determining the posterior pdf $p(\theta_k|y_{1:k})$ of the system parameters $\theta_k = \{\theta_{1k} \ \theta_{2k} \ \dots \ \theta_{pk}\}^T$ conditioned on the measurements $y_{1:k} = \{y_1 \ y_2 \ \dots \ y_k\}^T$ or the associated conditional mean and covariance given respectively by

$$a_{k|k} = \int \theta_k p(\theta_{1:p,k}|y_{1:k}) d\theta_k \quad (5a)$$

$$\Sigma_{k|k} = \int (\theta_k - a_{k|k})^T (\theta_k - a_{k|k}) p(\theta_k|y_{1:k}) d\theta_k. \quad (5b)$$

It may be noted that although the ‘process equations’ (Eq. (3)) are linear, the measurements (Eq. (4)) are nonlinearly dependent on the system states $\theta_i, i = 1, 2, \dots, p$. Consequently, the problem of DSE here is not amenable for closed form solution (via the Kalman filter) and one needs to either linearize the measurement model or employ particle filtering strategy to proceed further. In the present work we take the latter approach. Before we present the details of this formulation, it needs to be noted that, in further work, it is found expedient to add a small artificial noise to the process equation so that Eq. (3) is replaced by

$$\theta_{ik+1} = \theta_{ik} + w_{ik}; \quad i = 1, 2, \dots, p; \quad k = 1, 2, \dots, N_T. \quad (6)$$

Here $w_k = \{w_{ik}\}_{i=1}^p$ constitute a vector of random variable with joint pdf $p(w_k)$. It is also assumed that for $k = 1, 2, \dots, N_T$, w_k form a sequence of independent random vectors and this sequence is independent of $\xi_k, k = 1, 2, \dots, N_T$. As will be clarified later, this noise term facilitates the implementation of particle filtering, although, the statement that $\frac{d\theta_i}{d\tau} = 0; \theta_i(\tau = 0) = \theta_{i0}; i = 1, 2, \dots, p$; is free from any error. We would also like to point

out that the introduction of artificial noise “evolution” of time invariant system parameters is not new: such approaches have been discussed earlier by several authors; see, for example, the works of Liu and West [46], and Storvik [47], in the area of signal processing, and, the works of Yun and Shinozuka [33], Imai et al. [35], and Ghanem and Shinozuka [43] in the area of structural system identification.

3. Solution of the DSE problem

In the preceding section we have stated the problem of structural system identification in terms of a nonlinear filtering problem with the associated mathematical model for the structure being subsumed into the measurement equation. Based on the Markovian nature of Θ_k , and using Bayes’ theorem, it can be shown that the equations

$$p(\Theta_k | y_{1:k-1}) = \int p(\Theta_k | \Theta_{k-1}) p(\Theta_{k-1} | y_{1:k-1}) d\Theta_{k-1} \quad (7a)$$

$$p(\Theta_k | y_{1:k}) = \frac{p(y_k | \Theta_k) p(\Theta_k | y_{1:k-1})}{\int p(y_k | \Theta_k) p(\Theta_k | y_{1:k-1}) d\Theta_k} \quad (7b)$$

respectively represent the prediction and updation equations [22]. A solution to the DSE problem by using numerical quadrature on these equations is generally infeasible and Monte Carlo simulation strategies offer viable alternatives to deal with this problem. In the present study, we use the bootstrap particle filtering algorithm as developed by Gordon et al. [22] to tackle the filtering problem. The theoretical foundations of this method are based on an earlier result by Smith and Gelfand [53]. This result can be stated as follows: suppose that samples $\{x_k^*(i) : i = 1, 2, \dots, N\}$ are available from a continuous density function $G(x)$ and that samples are required from the pdf proportional to $L(x)G(x)$, where $L(x)$ is a known function. The theorem states that a sample drawn from the discrete distribution over $\{x_k^*(i) : i = 1, 2, \dots, N\}$ with probability mass function $L(x_k^*(i)) / \sum_{j=1}^N L(x_k^*(j))$ on $x_k^*(i)$, tends in distribution to the required density as $N \rightarrow \infty$. The algorithm for implementing the filter (with reference to Eqs. (3) and (4)) using N particles is as follows:

1. Set $k = 0$. Generate N samples $\{\Theta_{i,0}^*\}_{i=1}^N$ from the initial pdf $p(\Theta_0^*)$.
2. Generate $\{w_{i,k}\}_{i=1}^N$ from $p(w)$; generate $\{\Theta_{i,k+1}^*\}_{i=1}^N$ using Eq. (6). Set $k = k + 1$.
3. Run the FE codes that and generate $h_k[\Theta_{i,k}^*]_{i=1}^N$ and evaluate $p(y_k | \Theta_{i,k}^*)$.
4. Consider the k th measurement y_k . Define

$$q_i = \frac{p(y_k | h_k[\Theta_{i,k}^*])}{\sum_{j=1}^N p(y_k | h_k[\Theta_{j,k}^*])} \quad (8)$$

5. Define the probability mass function $P[\Theta_k(j) = \Theta_{i,k}^*] = q_i$; generate N samples $\{\Theta_{i,k}\}_{i=1}^N$ from this discrete distribution.
6. Evaluate

$$a_{k|k} = \frac{1}{N} \sum_{i=1}^N \Theta_{i,k} \quad (9a)$$

$$\Sigma_{k|k} = \frac{1}{N-1} \sum_{i=1}^N (\Theta_{i,k} - a_{k|k})^t (\Theta_{i,k} - a_{k|k}). \quad (9b)$$

7. Go to step 2 if $k < N_\tau$; otherwise, stop.

The central contention in the formulation of this algorithm is that the samples $\{\Theta_{i,k}\}_{i=1}^N$ drawn in step 4 above are approximately distributed as per the required pdf $p(\Theta_k | y_{1:k})$. The justification for this is provided by considering the updation Eq. (7b) in conjunction with the result due to Smith and Gelfand with $G(\Theta)$ identified with $p(\Theta_k | y_{1:k-1})$ and $L(\theta)$ with $p(\Theta_k | y_k)$. This filtering procedure is applicable to nonlinear process and measurement equations, and, non-Gaussian noise models. If the process ξ_k (Eq. (4)) is taken to be Gaussian with zero mean and covariance Σ_{ξ} , it follows that in step 2 above we use $p(y_k | \Theta_{i,k}^*) \sim N[h_k(\Theta_{i,k}^*), \Sigma_{\xi}]$. In the remaining part of the paper we designate the above filtering procedure as Method I. It may be noted that the presence of the artificial noise w_k in Eq. (6) ensures that the samples of Θ_k would not get frozen at their initial values drawn from $p(\Theta_0)$ and would evolve as k increases. In the numerical work it was empirically observed that noise levels with standard deviations less than about 0.5% of nominal values of Θ lead to reasonable results. Some recent studies in which the scope of the bootstrap particle filtering method has been explored in structural engineering applications are by Manohar and Roy [39], Nasrellah and Manohar [52] and Radhika and Manohar [54]. Fig. 1 shows the schematic of system identification procedure proposed in the present study.

Remarks.

- (i) The initiation of the filtering algorithm requires an assumption to be made on the initial form of the pdf $p(\Theta_0^*)$. In this study it is assumed that Θ_0 is uniformly distributed over a plausible range of values of its components and these components were taken to be independent. It was also found advantageous to draw samples using optimal space filling Latin hypercube sampling strategy [55] so that the initial guess distributes the sample points as uniformly distributed as possible within the chosen domain. It may be noted that the Matlab platform has readily available subroutines to implement this.
- (ii) To enhance the performance of the identification procedure, an additional step involving a global iteration is also employed in the present study. Here, the guess on pdf of Θ_0 is updated at the end of a given cycle of filtering by the final $p(\Theta_{N_\tau} | y_{1:N_\tau})$ and is used as the starting guess for the next cycle of filtering. This global iteration loop is repeated till a satisfactory convergence on the expected value of Θ conditioned on measurements is obtained. It may be noted that this step is fashioned after the earlier work of Hoshiya and Saito [34].
- (iii) The number of calls to the FE codes in step 2 depends upon the number of observation points N_τ and the major computational effort in implementing the algorithm is spent in this step. Bearing in mind that the problem of state estimation here essentially consists of estimating system parameters that are intrinsically time invariant, and, also, with a view to lessen the number of calls to the FE codes, the procedure listed above could be simplified as follows: We group the N_τ discrete values of τ into R groups with N_i number of discrete values of τ in the i -th group with $\sum_{i=1}^R N_i = N_\tau$. We assume that Θ_i remains constant for all values of τ lying within the i -th group. Also, the values of the probability measures q_i (in steps 3 and 4 above) are averaged over all values of τ within the i -th group. Accordingly, the filtering steps, using N particles, as per this modified procedure, are as follows:
 1. Set $r = 0$. Generate N samples $\{\Theta_{i,0}^*\}_{i=1}^N$ from the initial pdf $p(\Theta_0^*)$.
 2. Generate $\{w_i\}_{i=1}^N$ from $p(w)$.
 3. Evaluate $\{\Theta_{i,r+1}^*\}_{i=1}^N$ using $\Theta_{r+1} = \Theta_r + w_r$.
 4. Run FE codes and generate $h_k[\Theta_{i,r+1}^*]$ and evaluate $p(y_k | \Theta_{i,r}^*)$ for $(r-1)n_\tau \leq k \leq rn_\tau$ where $n_\tau = \frac{N_\tau}{R}$.

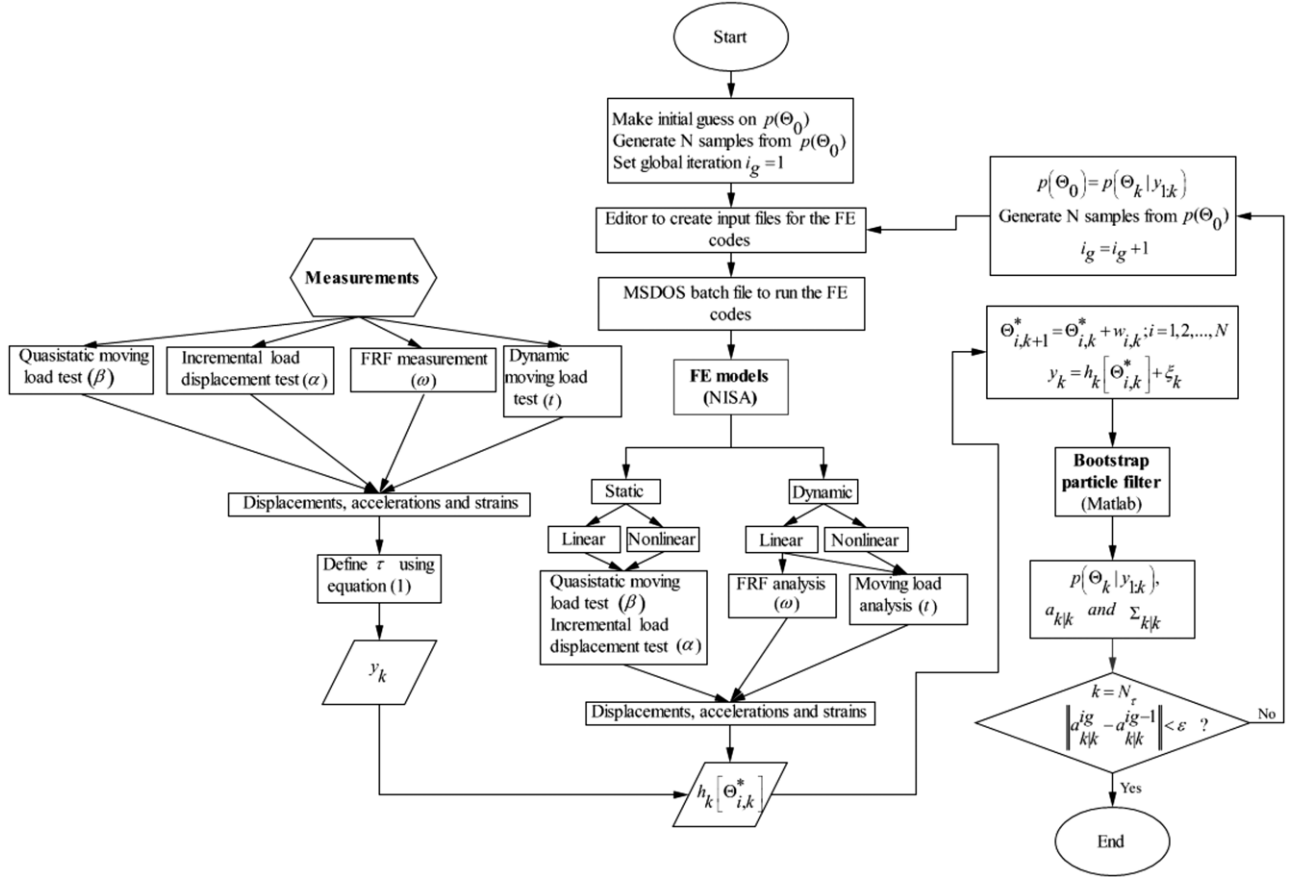


Fig. 1. Schematic of combined FEM and particle filtering strategy for structural system identification; detailed steps are outlined in Section 2.

5. Consider the k -th measurement y_k . Define

$$q_{k,j}^* = \frac{p(y_k | h_k[\Theta_{j,r}^*])}{\sum_{i=1}^N p(y_k | h_k[\Theta_{i,r}^*])}. \quad (10)$$

6. Evaluate $q_i = \frac{1}{n_r} \sum_{k=(r-1)n_r+1}^{rn_r} q_{k,i}^*$.

7. Define the probability mass function $P[\Theta_r(j) = \Theta_{i,r}^*] = q_i$. Generate N samples $(\Theta_{i,r})_{i=1}^N$ from this discrete distribution.

8. Evaluate

$$a_{r|r} = \frac{1}{N} \sum_{i=1}^N \Theta_{i,r} \quad (11a)$$

$$\Sigma_{r|r} = \frac{1}{N-1} \sum_{i=1}^N (\Theta_{i,r} - a_{r|r})^t (\Theta_{i,r} - a_{r|r}). \quad (11b)$$

9. Set $r = r + 1$ and go to step 2 if $r < R$; otherwise, stop.

In the numerical work, the above steps are combined with the global iteration step mentioned in item 2. We refer to the above modified filtering procedure as Method II in the rest of this paper.

4. Numerical examples

The formulation presented in the preceding sections is now exemplified by considering a suite of illustrations. The range of issues covered in these illustrations include: the use of synthetic measurement data, laboratory and field data; linear and nonlinear structural behavior; static and dynamic responses; combined use of data from more than one sensor type and more than one test scenario; and, identification of applied forces in conjunction

with unknown system parameters. The example structures consist of a rubber sheet with a hole undergoing large deformations, laboratory studies on single span beams and field studies on a multi-span masonry arch railroad bridge. In each of these examples, the structure in question is modeled using FEM on the NISA software platform and the particle filter algorithm is developed on the Matlab computational platform and these two disparate entities, along with the database of measurements, are made to interact automatically with each other through a set of batch files residing on the MSDOS platform (Fig. 1). In all the examples, the random vectors w_k and ξ_k are taken to be mutually independent and Gaussian distributed with zero mean and specified covariances. In making initial guess on pdf of Θ , the components of this vector are taken to be independent. All the computations were performed on a Pentium 4 computer with 2.1 GHz processor and 1 GB RAM.

4.1. Studies on a rectangular rubber sheet with a circular hole

Synthetic measurement data simulated from known numerical models and subsequently seeded with digitally simulated noise, offer useful means to assess the performance of the identification procedures. Since, the system parameters from which the measurements originate here are known, a measure of success of identification can be defined as $\zeta = \max_{1 \leq i \leq p} \frac{|\theta_i^{\text{ref}} - \theta_i^{\text{estimated}}|}{\theta_i^{\text{ref}}} \times 100\%$.

This measure facilitates the comparison of alternative identification methods and helps to gain preliminary confidence in identification procedures before they can be applied to real-life situations involving laboratory and field measurements and in which system parameters to be identified are essentially unknown and a measure like ζ cannot be defined.

Table 2

Example in Section 4.1; Numbers in parenthesis in columns 5–7 denote the % error in estimation of the parameters; the column on initial guess provides range of uniform distribution assumed for the initial pdf.

No	Parameter	Reference value	Initial guess	Estimate of the expected value of the system parameters		
				Case a	Case b	Case c
1	ρ (lb ⁴ /in ⁴)	1.2500E–03	(0.075E–03, 2.25E–03)	1.2453E–03 (0.38%)	–	1.2751E–03 (2.01%)
2	c_1 (psi)	25.0	(15, 45)	24.9108 (0.36%)	25.007 (0.03%)	25.6657 (2.66%)
3	P (lb/in ²)	90	(60, 180)	–	89.9940 (0.01%)	91.9914 (2.21%)

Here we consider the inverse problem of identifying parameters of a square rubber sheet with a central circular hole based on a few measured static and dynamic responses. An FE model that allows for large displacement and large strain responses is adopted and the analysis is based on total Lagrangian formulation with Newton Raphson iterations. The rubber sheet is modeled as made up of Mooney–Rivlin material. Fig. 2 shows the details of the problem considered; Fig. 2(a) shows the case of static loads on structure and Fig. 2(b) shows the FE model used. For the purpose of dynamic analysis we take $p(t) = 2250t$ lb/in² for $0 \leq t \leq 0.02$ s and $p(t) = 2250$ lb/in² for $t \geq 0.02$ s. The material properties of the structure include the following parameters: density (ρ), Mooney–Rivlin constants (c_1 and c_2) and Poisson's ratio (ν). This example structure has been employed earlier by Bathe et al. [56] to illustrate the capabilities of a FE nonlinear structural analysis code and, subsequently, for a similar purpose, by NISA code developers [57]. In the present study, based on the symmetry of the structure and the loading, we model 1/4 of the structure (Fig. 2(b)) and use 30 number of 4-noded quadrilateral plane stress elements which results in a model with 42 degrees of freedom (dof-s). The system parameters to be identified are taken to be ρ and c_1 ; additionally, the magnitude of the applied static pressure (P) is also considered as an unknown to be identified. It is important to note that the FE modeling and solution capabilities already exist in the FE software being used and the proposed identification algorithm takes advantage of these readily available features. The following cases are considered: (a) Case a: Identification of ρ and c_1 based on measurement of dynamic displacements and accelerations under the action of transient dynamic load given by $p(t) = 2250t$ lb/in² for $0 \leq t \leq 0.02$ s and $p(t) = 2250$ lb/in² for $t \geq 0.02$ s; (b) Case b: Identification of c_1 and P based on measurement of displacements under the static pressure load (Fig. 2(a)); (c) Case c: Identification of ρ , c_1 and P based on combined use of two episodes of measurements: one under static loads (Fig. 2(a)) and the other under dynamic loads (as in Case a). The measured quantities include displacements for static case and additional measurements of accelerations for the dynamic case.

For Cases a and c, measurements on displacements and accelerations in the x -direction at nodes 1, 2, 3, 4, 5, 6, 22, 23, 24, 25, 26, 27, 36 and displacements and accelerations in the y -direction at nodes 2, 3, 4, 5, 6, 7, 23, 24, 25, 26, 27, 28, 42 are made. For Case b, the above mentioned displacement components are measured. The particle filtering algorithm employed 150 particles and the standard deviation of elements of noise vector w_k was assumed to be 0.04% of the respective nominal values. Similarly, the standard deviation of components of ξ_k was assumed to be 4% of the noise free responses. Table 2 summarizes the results of identification for Cases a–c. The table also provides the values of the system parameters of the reference structure from which the measurements are synthetically generated and also the details of initial guess made on $p(\theta_0)$. In dealing with dynamic measurement data it was found advantageous to use Method II for filtering. In fact, Case a was solved using both Methods I and II with $R = 1$. As per Method I it was found that at the end of first global iteration, the estimate of ρ was $1.2547E-03$ lb⁴/in⁴ and this was obtained using 151 calls to the FE code (that is, maximum value

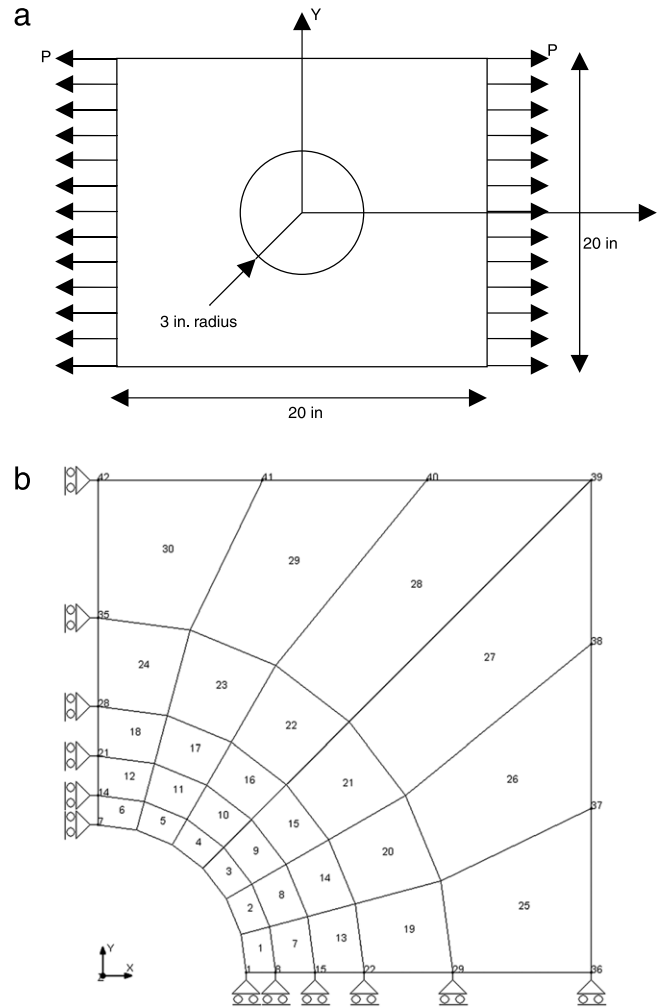


Fig. 2. Example 4.1; (a) a rectangular rubber sheet with a central circular hole subjected to tensile pressure; (b) finite element model for quarter of the structure.

of k was 151). On the other hand, with 10 iterations, Method II lead to the estimate of $\rho = 1.2363E-03$ lb⁴/in⁴ which involved only 10 calls to the FE code. The results shown in Table 2 are based on Method II with $R = 1$ so that $n_t = N_t$. It may be noticed that the identification procedure is fairly successful with a maximum error of 2.66% occurring in the estimation of constant c_1 in Case c. Fig. 3(a) and (b) show the evolution of conditional mean and standard deviation of one of the system parameters, namely, c_1 , (for Case c) as a function of the global iteration number. It may be observed that the iterations in this case converge in about 10 iterations and a similar feature was also observed for estimation of other constants (ρ and P). Fig. 4(a) and (b) show the pdf-s of the initial guess on c_1 (for Cases a and c) along with the pdf-s at the end of identification process. The results on prediction of system response from the identified system along with the corresponding measurement and results from the initially guessed model are shown in Fig. 5. The satisfactory performance of the identification

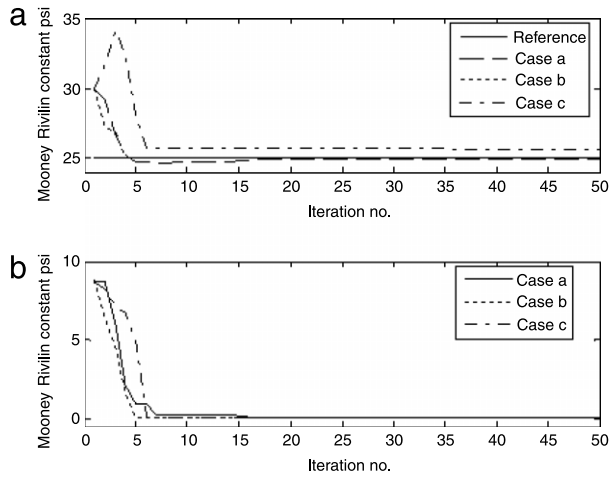


Fig. 3. Example 4.1; Estimation of Mooney–Rivlin constant (a) expected value of c_1 (Method II); (b) standard deviation of c_1 (Method II).

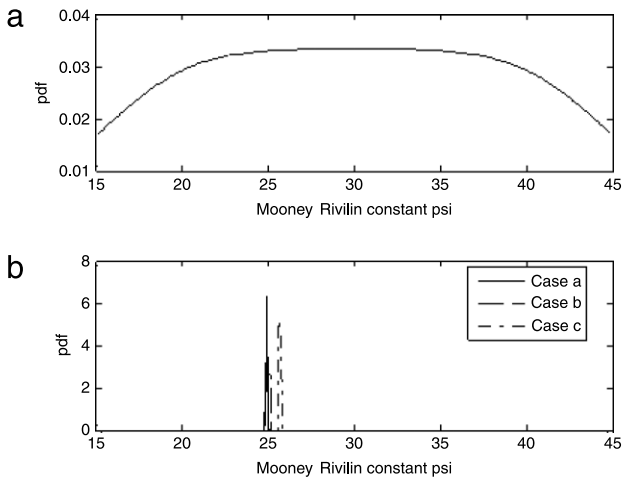


Fig. 4. Example 4.1; (a) pdf of the initial guess on c_1 ; (b) pdf of c_1 at the end of identification procedure.

algorithm is evident from these results. The computational times needed to run Cases a, b and c, for one cycle of global iteration with 150 particles, was about 129 s, 109 s and 156 s respectively.

4.2. Laboratory experiments on beam structures

In this example we consider measurement data from laboratory experiments on a beam structure (Fig. 6). The beam essentially consists of a main central span with slight overhangs at the two ends. The beam specimen studied was made up of steel with rectangular cross section of constant thickness. However the beam width was varied over its length by dividing the beam into 12 segments and the beam width was varied across these segments while remaining constant within a segment. For the beam specimen used in the study these widths were measured respectively to be 50.06, 50.03, 47.00, 44.91, 44.13, 46.17, 47.18, 45.01, 47.87, 48.79, 49.97 and 49.96 mm. The beam was fixed near the two ends using a screw-bolt arrangement. This lead to slight overhangs at the two ends as shown in Fig. 6(b). In developing the FE model, the possible partial fixity conditions at the supports was simulated by adding rotary springs at the supports (Fig. 6(b)). Two types of experiments were conducted on this beam:

- (i) Case a: here a concentrated force of magnitude 46.73 N was made to move quasistatically across the length of the beam and beam response was measured for each location of the applied

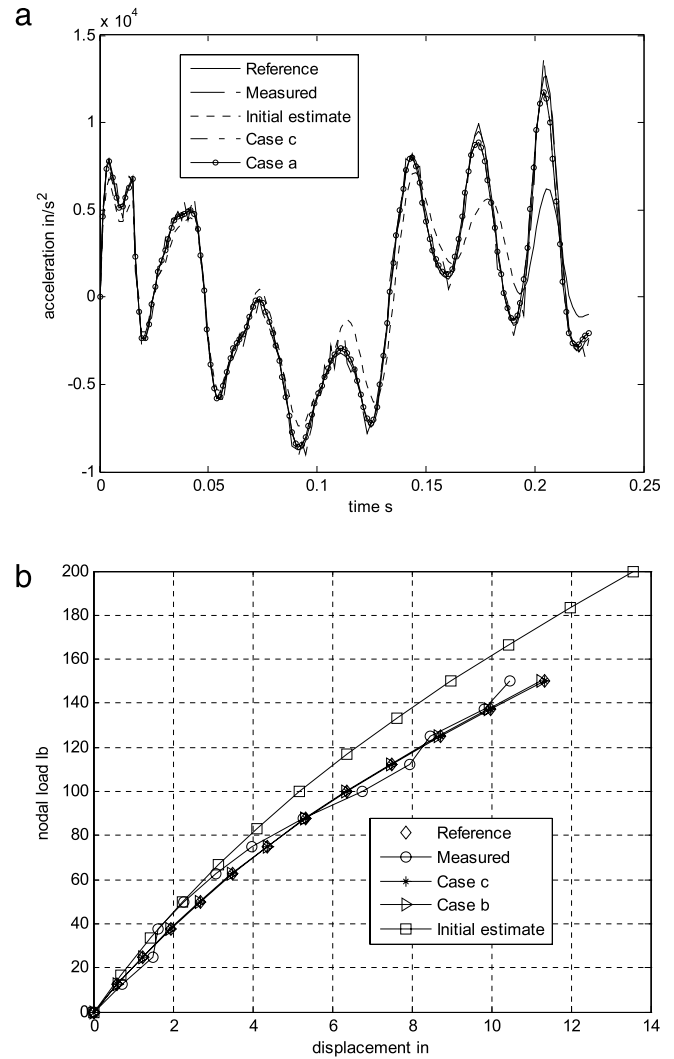


Fig. 5. Example 4.1; Prediction on system response from identified and initial models (a) acceleration x-direction at node 36; (b) displacement in x-direction at node 36.

load; nine locations for the load were used with the load position measured from the left support being 0.1930, 0.3130, 0.4330, 0.5530, 0.6730, 0.7930, 0.9130, 1.0330 and 1.1530 m.

- (ii) Case b: here a concentrated force was applied statically at 0.673 m from the left end and the magnitude of the load was incremented in 6 steps with load at these steps being, respectively, 2.22 N, 11.12 N, 20.03 N, 28.88 N, 37.83 N, 46.73 N; the beam response was measured for each magnitude of the applied load.

In beam was instrumented with 10 number of strain gauges (mounted on the top fibre of the beam) and two LVDT-s mounted at a distance of 0.613 and 0.853 m from the beam left-end (Fig. 6(a)). For each episode of loading response were measured 10 different times. The identification problem here consists of determining the flexural rigidities of the 12 beam segments $\{EI\}_{i=1}^{12}$ and the two spring constants k_{θ_1} and k_{θ_2} at the two supports. This problem has been earlier studied by the present authors [52] using the particle filter based approach but based on an FE model (developed using the Matlab platform) using Euler–Bernoulli beam elements. Here we re-consider the problem using the approach schematized in Fig. 1 and we use 26-dof FE model (residing on the NISA software) that uses Timoshenko beam elements. The beam parameters $\{EI\}_{i=1}^{12}$ here are essentially unknown; however, a reasonable estimate for these quantities can be obtained by actual

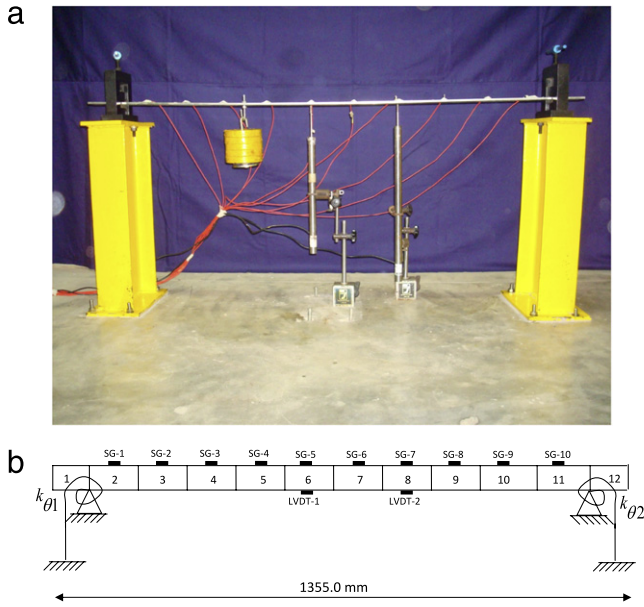


Fig. 6. Example 4.2; (a) experimental set up showing sensors and applied loads; (b) location of strain gauges (SG1 to SG10) and LVDT-s (1 and 2).

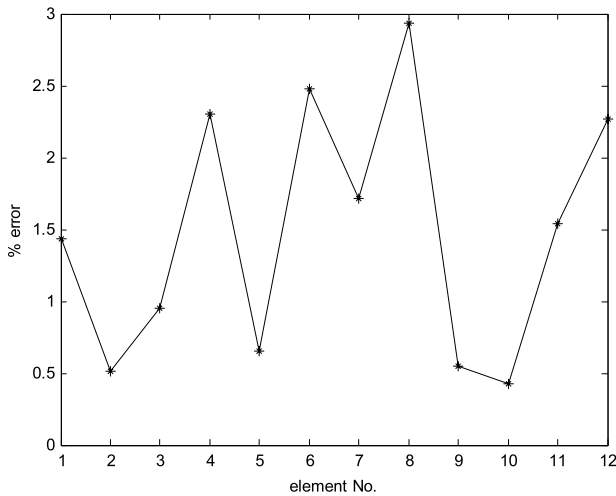


Fig. 7. Example 4.2; Notional error parameter for the Young's moduli in the 12 segments of the beam.

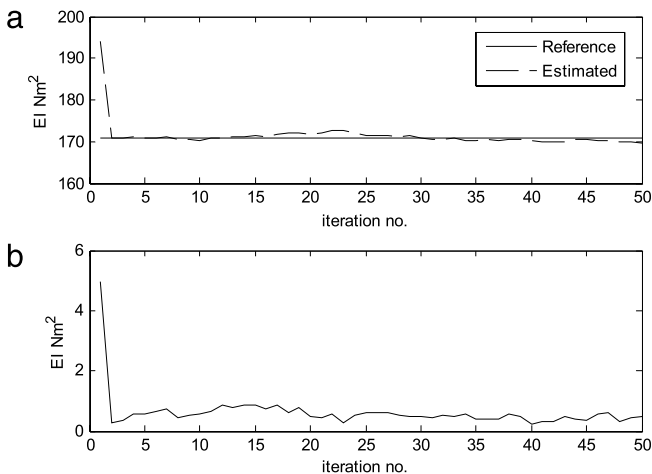


Fig. 8. Example 4.2; Estimation of Young's moduli and joint stiffness at supports; (a) conditional expectation of EI_5 ; (b) conditional standard deviation of EI_5 .

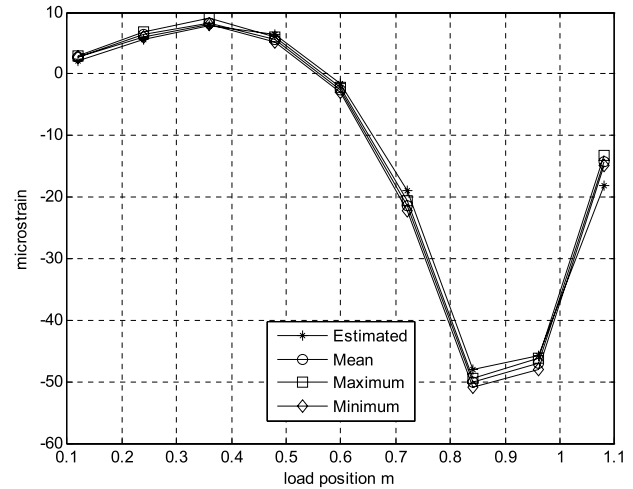


Fig. 9. Comparison of measured response with predictions from the identified model; response at strain gauge SG-7 under quasistatic moving load test.

measurement of the cross sectional properties and by assuming Young's modulus of the material (steel) as $2.1 \times 10^{11} \text{ N/m}^2$. This enables the notional definition of an error parameter as $\frac{|E|_{\text{exact}} - |E|_{\text{estimated}}}{|E|_{\text{exact}}} \times 100\%$ and the plot of this error is shown in Fig. 7. The identification procedure here is based on the data from measurement Case a (quasistatic moving load case) and is based on the use of 200 particles. The various noise terms assumed here are as follows: standard deviation of noise in strain gauges SG-1-SG-10 are respectively: 2.3, 1.02, 0.71, 1.40, 1.40, 1.83, 1.35, 0.66, 1.03 and $2.38 \mu\text{strain}$; LVDT-1 and LVDT-2: 0.03 mm. These noise levels approximately corresponded up to about 4% and 2% of maximum measured responses in each strain gauges and LVDT-s respectively. From Fig. 7 it is seen that the highest notional error is less than 3%. It is important to note that these error measures cannot be defined for parameters k_{θ_1} and k_{θ_2} since no reasonable guess can be made on their true values. In the numerical work, the expected values of these parameters were obtained as 8.7747×10^3 and $1.1134 \times 10^4 \text{ N m/rad}$ and the corresponding standard deviations were 33.7030 and 31.3740 N m/rad. Fig. 8 show trajectories of the conditional expectation and standard deviation of EI_5 as a function of global iteration number. The system parameters were observed to converge in about 50 iteration steps. Fig. 9 shows the prediction of system response based on the identified model, along with the measured response (measurement Case a). The data on measured response are shown in terms of mean and range over 10 episodes of measurements. Here again, the identification of system parameters is deemed to be satisfactory. The computation time for running cases a and b, for one cycle of global iteration with 200 particles, were about 913 s and 620 s respectively.

4.3. Field investigations on a multi-span arch bridge

The present authors are part of a team that is conducting studies on condition assessment of a few existing railway bridges in India. The goal of these studies have been to assess the capability of existing bridges to carry increased axle loads, longer train formations and higher formation speeds. As a part of these studies, five existing bridges in South India have been extensively instrumented and bridge response to a suite of static/dynamic loads resulting from moving train formations have been measured. The loads here are either diagnostic in nature (their spatial distribution, speeds and magnitudes are measured) or due to ambient train traffic (when load characteristics are not precisely known). Problems of structural system identification

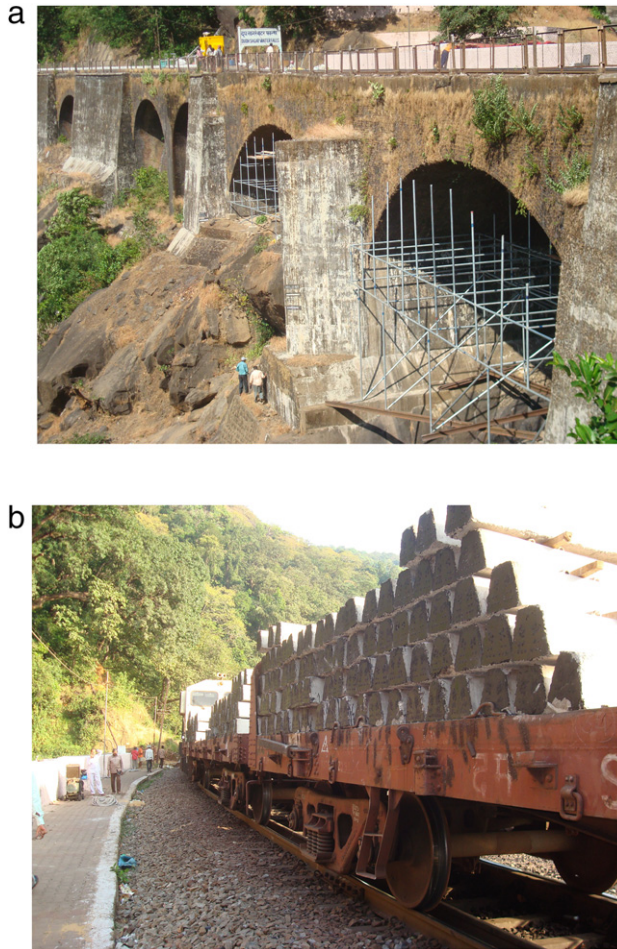


Fig. 10. Example 4.3; (a) 5-span masonry arch bridge; note that three smaller spans (appearing towards the left top corner) are closed and only two spans are active; the temporary tube structure below the arch spans were constructed to gain access for placement of sensors; (b) sleeper loaded BFR wagons used in static and dynamic load tests.

arise prominently in these studies and, in this section, we describe one such problem with reference to a multi-span brick masonry arch bridge and illustrate the application of identification procedure developed in this study for this problem.

The bridge under consideration is a 120-year old, five span, masonry arch bridge with stone masonry piers and abutments, brick masonry arch barrels and filler material made up of graded soil (bridge no. 128 in the South-Western Division of Indian Railways; Fig. 10). The bridge spans are 7.70, 7.70, 7.70, 17.71, and 17.30 m; the first three smaller spans have been filled up and closed and only two main spans (17.71 and 17.30 m) remain operational (Fig. 10(a)). The bridge lies on a hilly terrain on a slope of 1:30 along the longitudinal direction. The two operational spans form the focus of the present study. These two spans were instrumented with strain gauges (20 numbers), LVDT-s (6 numbers), tilt meter (1 number) and uniaxial /multiaxial accelerometers (10 number of channels). The bridge response was monitored over a period of about 96 h and extensive data have been collected under various loading scenarios. One of the diagnostic tests that was performed consisted of loading the bridge with a test formation of known weights and geometry. Fig. 11 shows the formation which consists of four locomotives (each having six axles, two in front and two in the rear; locomotive types: WDG4 and WDG3A) and four wagons (two Boxen and two BFR wagons each having four axles). The formation has a total of 40 axles and Fig. 11 shows the axle loads inferred from measured weights of each formation unit. The Boxen

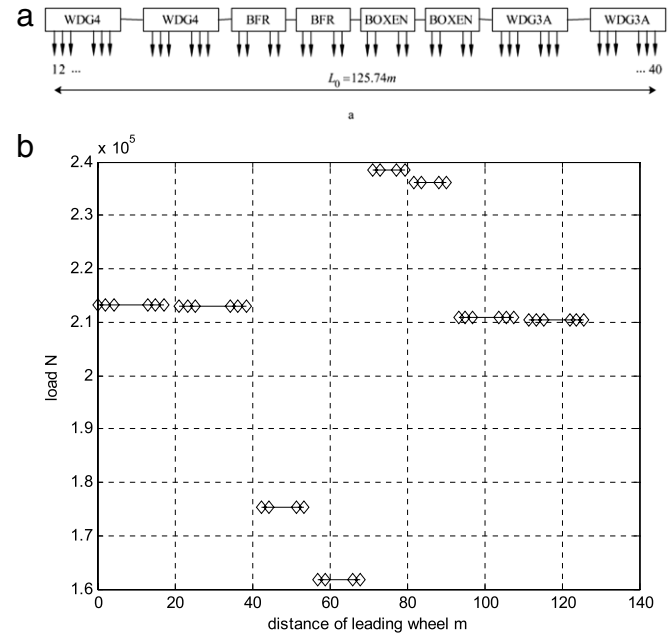


Fig. 11. Example 4.3; (a) schematic of formation used in quasistatic moving load tests; WDG4 and WDG3A are locomotives; BFR: open roof wagons carrying known number of prestressed concrete sleepers; BOXEN: closed roof wagons carrying iron ore of known weights; the formation has 40 axles and these are numbered as 1, 2, ..., 40; (b) the magnitude of axle loads and wheel distances.

wagons were loaded with iron ore while each of the BFR wagons were loaded with up to 200 numbers of prestressed concrete sleepers (each sleeper weighing 2800 N; Fig. 10(b)). The following tests were conducted.

- Case a: the formation was made to move with known speeds on the bridge from left-right and right-left and for each passage of the load, the bridge responses were measured.
- Case b: the formation moved quasistatically on the bridge so that it was made to halt on the bridge whenever an axle crossed a reference point ('rp') marked on the rail at the left springing level (Fig. 12).
- Case c: The axle loads transferred from the BFR wagons (carrying prestressed concrete sleepers) was made to vary by changing the number of sleepers that were placed on the wagon. For each case of loading, the formation was made to halt in precisely an identical way and the static response of the bridge was measured.

In the present study we focus on measurements from Case b and apply the identification algorithm developed in the present paper to estimate the system parameters. The following are some of the salient features of this investigation:

- The position of the leading axle was treated as the artificial independent variable (parameter a in Section 2) and $\tau = a/L_0$ where L_0 is the length of the formation (Fig. 11). Thus, given that the formation has 40 axles, the number of loading episodes, and hence the possible number of distinct values that the variable τ can take is 40.
- Two alternative FE models were considered: one included the 3-dimensional behavior of the structure and used 6-noded brick elements with 3-dof-s per node, and the second, was a 2-dimensional model based on the use of 4-noded quadrilateral elements with 2-dof-s per node. By investigating the prediction from these two models on system response due to a set of quasi-static moving loads, and also based on demands on computational efforts, it was decided that

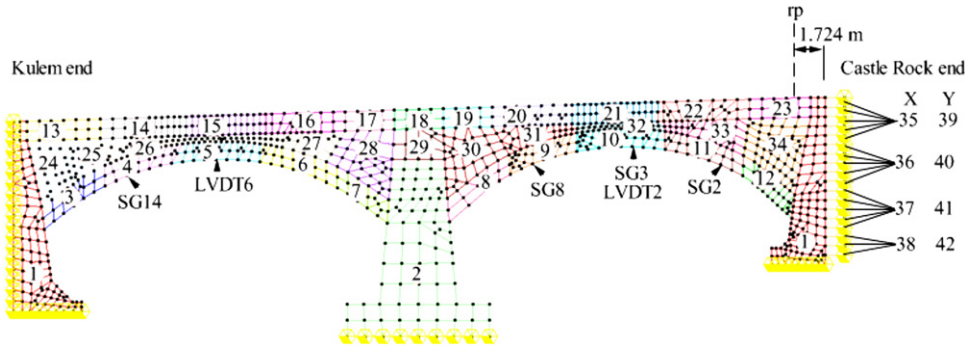


Fig. 12. Example 4.3; Plane stress FE model for the bridge structure; the numbers in circles correspond to zones used in identification process; five strain gauges and two LVDT-s used in the present study are also shown; the point 'rp' shown on the figure corresponds to the reference point used in the quasistatic moving load test.

the 2-dimensional model using plane stress finite elements could form the basis for the identification algorithm. The model that was used had 2230 number of dof-s (Fig. 12). As has been already mentioned, of the five spans that the bridge had, three arch spans were closed and they did not offer structural resistance through the arch action. Therefore the model was limited to the study of the two operational spans and accordingly only two spans were modeled for FE analysis (Fig. 12). However, to include the inevitable effects that the inactive arch spans would have on the active spans, the boundary conditions at the interface were represented through a set of discrete two-dimensional springs (16 numbers). The FE model thus consisted broadly of five major entities: two arch barrels, abutments, pier, discrete springs at one end, outer filler material (consisting of rails, ballast, sleepers and sandy soil) and inner soil layer (consisting of sandy soil).

- (iii) For the purpose of parameter identification, the bridge structure was divided into 42 zones such that within each zone the structural parameters were taken to be constant (Fig. 12). Thus, the arch barrel was divided into 10 zones and the outer and fillers each into 11 zones. A set of 8 discrete springs in x and y directions were used to represent the partial fixity condition at one of the ends. The two piers were taken to lie in the same zone and abutment was classified as a separate zone. The Young's modulus and Poisson's ratio within each zone in the arch barrel, fillers, abutment and piers and the discrete springs at the end were taken to be the system parameters to be identified. Thus the total number of parameters to be identified was 76.
- (iv) Fig. 12 also shows the various sensors that were used in the present study. This consisted to 4 strain gauges and two LVDT-s. The structure was indeed instrumented with several other sensors but the sensors listed above provided data that could be employed in SSI using 2-dimensional FE model.
- (v) The standard deviation of noise in strain gauges SG-2, SG-3, SG-8 and SG-14 were taken to be respectively 2.4724, 0.6820, 1.7043, and 6.0715 μ strain; similarly, the standard deviation of noise in LVDT-2 and LVDT-6 were taken to be 0.0882 mm and 0.0746 mm respectively. These noise levels approximately corresponded up to about 10% of maximum measured responses in each of the strain gauges and LVDT-s. The standard deviation of the noise process w_k was taken to be 0.5% of the nominal values of the respective system parameters.
- (vi) The filtering algorithm was implemented with 100 particles and up to 100 numbers of global iterations were performed.

Fig. 13 shows the evolution of one of the system parameters (Young's modulus of the arch barrel) as a function of the global

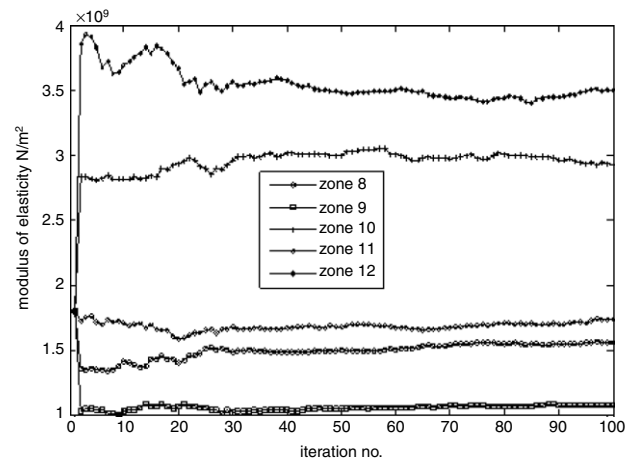


Fig. 13. Example 4.3; Estimation of system parameters for the arch bridge problem; results for Young's modulus of the arch barrel.

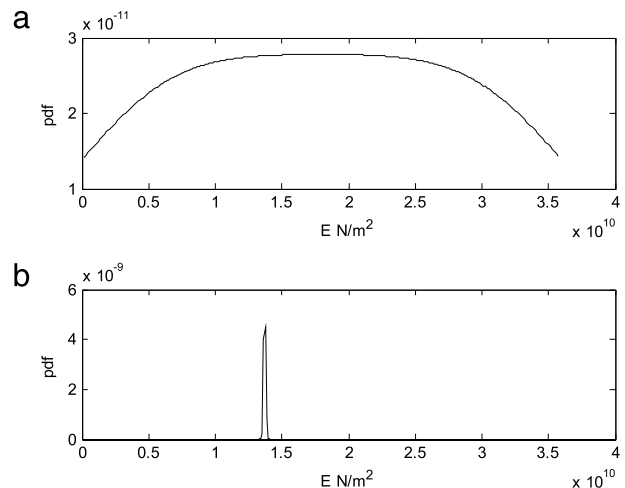


Fig. 14. Example 4.3; (a) pdf of the initial guess on Young's modulus of zone 1; (b) pdf of Young's modulus of zone 1 at the end of identification procedure.

iterations. The initial guess on pdf-s of the system parameters is summarized in Table 3 and Fig. 14 shows the result on final pdf along with the initial guess for one of the system parameters. Tables 4 and 5 summarize the conditional mean and standard deviation of the 76 system parameters. After the identification process was completed, the identified system properties were also averaged spatially within a bridge part (e.g., arch barrel,

Table 3

Example 4.3; Details of the initial guess on pdf of system parameters; the system parameters were assumed to be uniformly distributed and this table provides the range over which the variables were taken to be uniformly distributed.

No.	Item	E (Pa)		μ	
		E_{\min}	E_{\max}	μ_{\min}	μ_{\max}
1	Pier	3.1008e+008	3.5904e+010	0.0026	0.3988
2	Abutments	3.1888e+008	3.5909e+010	9.5178e−004	0.3974
3	Arch barrel	1.5238e+006	3.5964e+009	1.7447e−004	0.3998
4	Outer filler	2.4246e+007	1.9995e+010	1.5740e−005	0.2996
5	Inner filler	1.1365e+005	1.5981e+008	1.6693e−005	0.2999
6	Springs	8.5059e+006	9.9914e+009	–	–

Table 4

Example 4.3; Mean and standard deviation of the system parameters estimated using 100 particles.

Zone	Zone no.	Estimate of Young's modulus E (Pa)				Estimate of Poisson's ratio μ			
		Mean	Standard deviation	Spatial average of mean	Spatial average of standard deviation	Mean	Standard deviation	Spatial average of mean	Spatial average of standard deviation
Pier, abutments	1	1.37E+10	6.03E+07	1.78E+10	6.32E+07	4.03E−01	1.17E−03	3.24E−01	1.38E−03
	2	2.20E+10	6.62E+07			2.45E−01	1.60E−03		
	3	3.81E+09	1.03E+07			3.30E−01	1.50E−03		
	4	1.58E+09	3.35E+06			1.53E−01	3.85E−04		
	5	1.21E+09	3.47E+06			8.86E−03	3.71E−05		
	6	1.61E+08	6.34E+05			3.18E−01	1.06E−03		
Arch barrel	7	1.36E+09	6.39E+06	1.89E+09	6.75E+06	1.29E−01	3.73E−04	2.03E−01	9.70E−04
	8	1.56E+09	6.61E+06			3.26E−01	1.65E−03		
	9	1.08E+09	3.66E+06			2.38E−01	8.70E−04		
	10	2.93E+09	7.94E+06			9.80E−03	5.93E−05		
	11	1.74E+09	4.51E+06			2.85E−01	2.80E−03		
	12	3.50E+09	2.05E+07			2.34E−01	9.66E−04		
Outer filler	13	1.08E+10	2.60E+07	9.99E+09	3.93E+07	9.05E−02	2.90E−04	1.16E−01	5.78E−04
	14	4.16E+09	1.51E+07			1.51E−01	4.86E−04		
	15	5.70E+09	2.09E+07			2.62E−01	2.84E−03		
	16	1.91E+10	7.27E+07			8.62E−02	2.76E−04		
	17	1.47E+10	6.35E+07			8.22E−02	3.30E−04		
	18	1.26E+10	8.77E+07			1.18E−01	3.59E−04		
	19	1.61E+10	7.91E+07			3.02E−02	2.07E−04		
	20	4.92E+08	1.10E+06			2.04E−02	1.94E−04		
	21	4.49E+09	1.55E+07			1.41E−01	5.42E−04		
	22	1.45E+09	3.26E+06			2.73E−01	7.62E−04		
	23	2.04E+10	4.78E+07			2.70E−02	7.59E−05		
	24	3.49E+08	1.18E+06			2.48E−01	1.01E−03		
Inner filler	25	3.06E+08	2.55E+06	2.62E+08	1.36E+06	1.13E−01	3.19E−04	1.93E−01	9.41E−04
	26	2.82E+08	1.24E+06			2.41E−01	1.80E−03		
	27	1.74E+08	8.97E+05			2.22E−01	6.74E−04		
	28	1.10E+07	5.89E+04			2.02E−01	5.53E−04		
	29	2.57E+08	1.71E+06			1.72E−01	7.95E−04		
	30	8.24E+07	3.51E+05			2.48E−01	1.81E−03		
	31	3.25E+08	1.56E+06			1.92E−01	7.26E−04		
	32	3.69E+08	1.69E+06			2.31E−01	1.74E−03		
	33	3.30E+08	1.87E+06			2.11E−01	8.17E−04		
	34	3.99E+08	1.86E+06			3.93E−02	1.12E−04		

Table 5

Example 4.3; Mean and standard deviation of the system parameters estimated using 100 particles.

Zone	Zone no.	Estimate of springs constants (N/m)			
		Mean	Standard deviation	Spatial average of mean	Spatial average of standard deviation
Springs in x-direction	35	1.89E+09	6.99E+06	3.54E+09	9.50E+06
	36	8.28E+09	1.78E+07		
	37	1.21E+09	3.17E+06		
	38	2.80E+09	1.01E+07		
Springs in y-direction	39	7.03E+09	4.32E+07	8.34E+09	3.79E+07
	40	1.57E+09	6.25E+06		
	41	9.65E+09	3.26E+07		
	42	8.31E+09	5.60E+07		

inner filler etc.) and these averages are also provided in Tables 4 and 5. The prediction of a few bridge responses from the identified model and the initial model are compared with field

measurements in Fig. 15(a) and (b). Clearly, at the end of data assimilation, the prediction from the initial model gradually moves towards the measured values thereby indicating the satisfactory

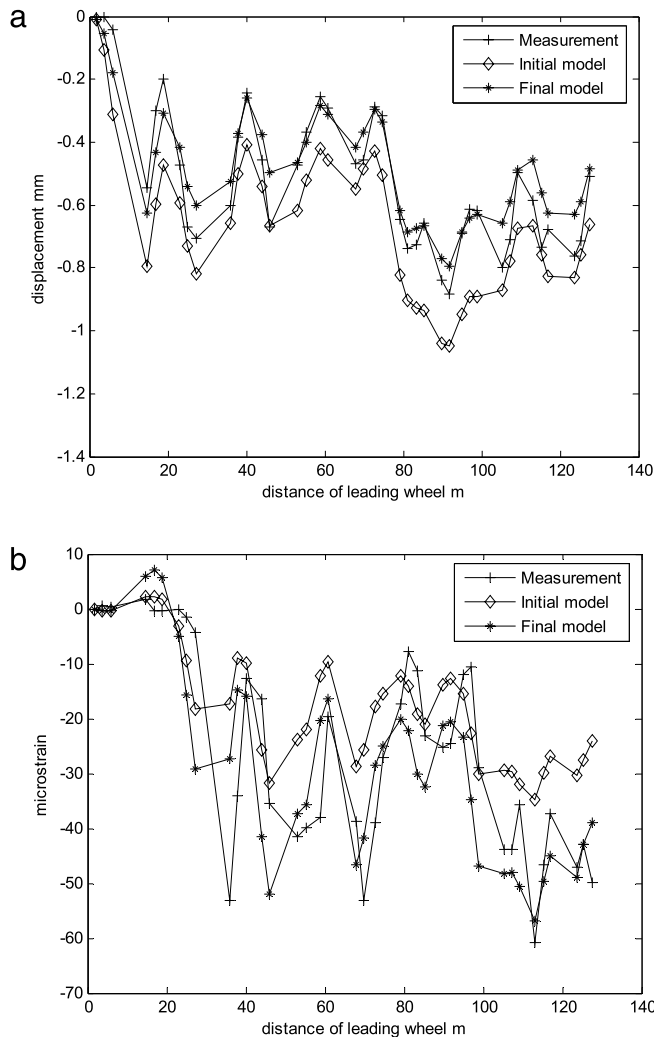


Fig. 15. Example 4.3; Comparison of predictions on system response from identified and initial models with corresponding measurements; (a) LVDT-2; (b) SG-14.

performance of the identification procedure. The implementation of the identification algorithm was time intensive and one cycle of global iteration with 100 particles requiring about 5.8 h of CPU.

Remarks.

1. From Table 3 it may be observed that the initial guesses on pdf of the Young's modulus of material in different parts of the bridge are taken to span a wide range (2–4 decades) and, notwithstanding this wide range, the identification algorithm performs reasonably well and provides acceptable estimates to the system parameters. This would mean that the initial guess on the system parameters need not be close to the final solutions.
2. In implementing the identification algorithm the structure is divided into 42 zones. During the early part of our studies, we had assumed that each of the bridge units (arch barrel, piers, abutment and fillers) have identical parameters. In this case, however, the identification procedure was observed to perform poorly presumably because the parameterization here did not provide sufficient room for the algorithm to explore different combinations of system parameter values during the data assimilation process. The zonation used subsequently clearly enabled this possibility. A detailed zonation could be eventually followed up by spatial averaging (within each bridge unit), as has been done in Tables 4 and 5. The resulting structure, with

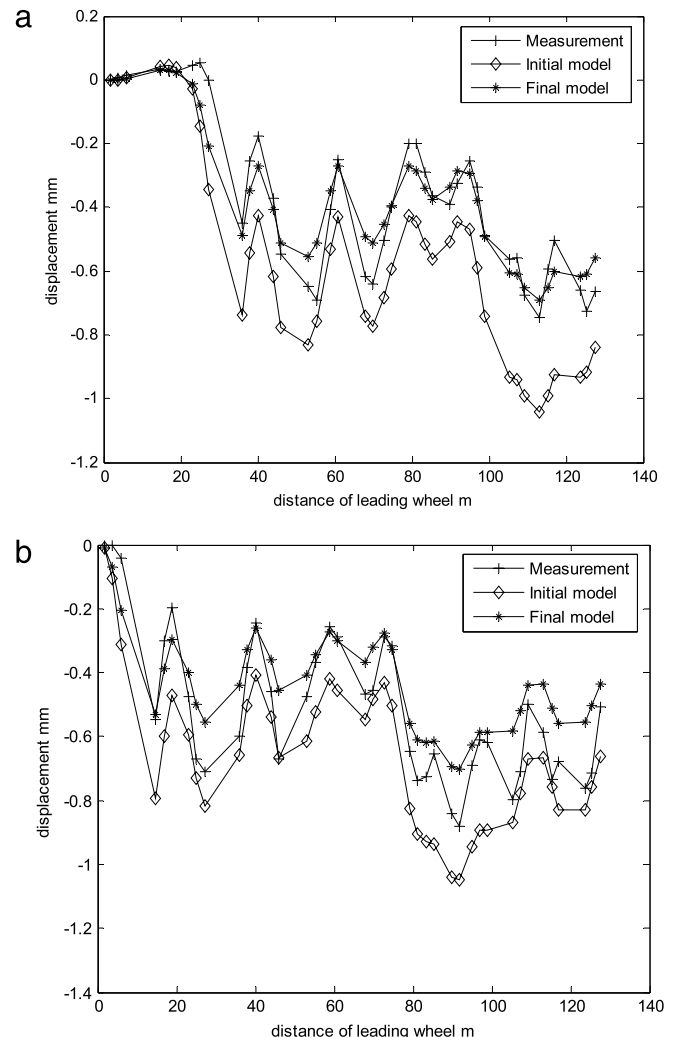


Fig. 16. Example 4.3; Comparison of model predictions based on spatially averaged system parameters and measurements (a) LVDT-6; (b) LVDT-2.

these spatially averaged properties, could as well be deemed as the model suitable for further predictions. To demonstrate this we have also compared the prediction from such a model with measured responses under quasistatic moving loads (Fig. 16(a) and (b)) and these results show reasonably good mutual agreement.

3. Based on the structural model with parameters identified as above, the bridge response to incrementally applied static loads (test scenario: Case c) was predicted with a view to compare these predictions with measured responses. The model predictions on displacements at midspans (LVDT-2 and LVDT-6) and strain at quarter point are compared with corresponding measurements and they are seen to show reasonably good mutual agreement (see Table 6).
4. As has been already noted, measurements on dynamic response of the bridge under passage of the formation (Fig. 11) with known speeds were also made. These data could be utilized to identify dynamic characteristics of the bridge structure. We have not included this aspect of the study in the present paper. However the stiffness parameters identified using static tests could be used in conjunction with assumptions on mass and damping properties to predict the dynamic response of the bridge under the passage of dynamically moving loads. To illustrate this we assume that the density of material in pier, abutment, ring and outer filler are 2300 kg/m^3 and density

Table 6

Example 4.3; Comparison of model predictions and measured responses under incrementally varied static load test; note that each sleeper weighed 2800 N and the self-weight of the wagons were 229.36 and 283.50 kN; refer to Fig. 12 for location of LVDT2, LVDT6 and SG2.

Load →		184 sleepers	200 sleepers
LVDT2	Measured (mm)	−0.5500	−0.5700
	Estimated (mm)	−0.6447	−0.6721
LVDT6	Measured (mm)	−0.6000	−0.6000
	Estimated (mm)	−0.5634	−0.5910
SG2	Measured (μstrain)	−10.9000	−12.3000
	Estimated (μstrain)	−11.9222	−12.7443

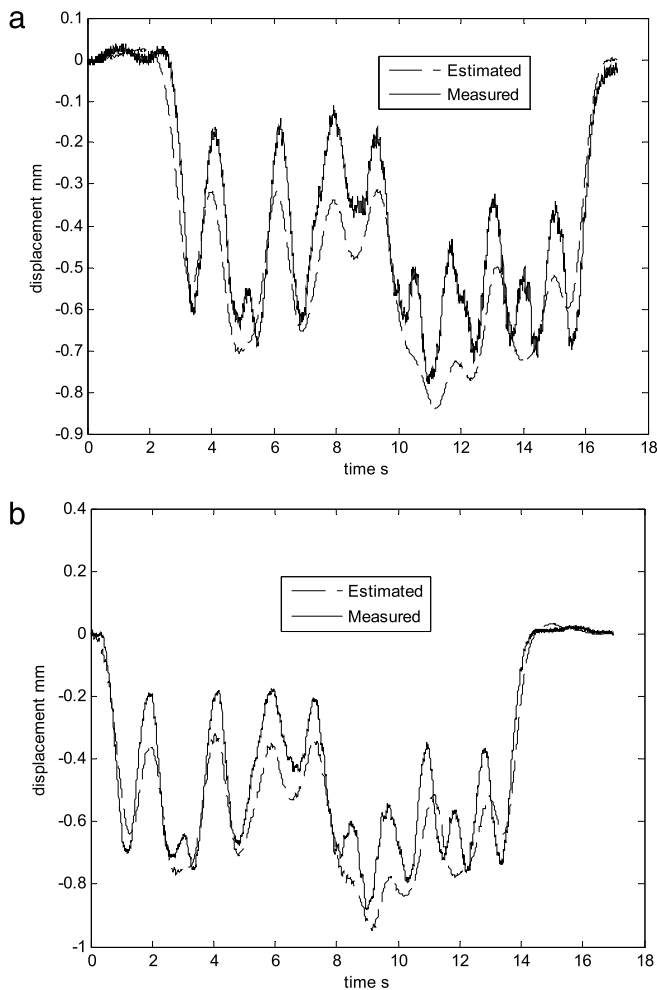


Fig. 17. Example 4.3; Comparison of model predictions and measurements when the formation in Fig. 12 cross the bridge at 38 kmph; (a) LVDT-6; (b) LVDT-2.

of inner core is 1800 kg/m^3 . The damping in the structure is assumed to be such that 3% of modal strain energies in piers, abutments and arch barrel dissipated via damping and 6% of energies in outer and inner fillers is similarly dissipated. Fig. 17 compares the model predictions on midspan transverse displacements with corresponding measurements when the formation shown in Fig. 11 crosses the bridge at 38 kmph. The results show good qualitative agreement. It may be noted that in the analytical prediction, the possibility of dynamic interactions between moving vehicle and bridge structure is neglected and this assumption is perhaps reasonable since the total mass of the arch barrel and filler was estimated to be about $1030\text{E}+03 \text{ kg}$ which was considerably higher than the mass of the moving vehicle (when it completely occupies the bridge span) which was around $305\text{E}+03 \text{ kg}$.

5. Closing remarks

The present study develops an identification procedure that combines finite element method for structural modeling with Monte Carlo simulation based dynamic state estimation techniques. Given the versatility of these two techniques in their ability to handle large scale structural models, nonlinear structural behavior, action of static and dynamic loads, and uncertainties in measurements and modeling, the identification procedure developed in this study has wide ranging capabilities. The DSE methods have the capability to perform in real time but this feature is not of particular relevance in the problems considered in this study. A key feature of the proposed method is the introduction of a dummy independent variable that facilitates assimilation of static and (or) dynamic measurement data from multiple sensors and multiple test scenarios in a unified manner. This variable also enables pseudo-sequencing of measurements even when these data originate from static tests. The procedure developed readily uses the capabilities of professional finite element softwares with no need to recast governing equations in state space form or to discretize them using specialized techniques. Computational requirements, such as calculation of sensitivities or application of regularization techniques, as are needed in many other identification procedures, are avoided in this formulation. Satisfactory performance of the procedure developed has been illustrated with the help of linear and nonlinear structural models and using measurement data that originate from computational models, laboratory experiments and field studies. The computational performance of the identification method can be improved by embedding the identification tools within FE softwares and by parallelizing the computation. Work on these lines is being currently pursued by the present authors.

The performance of the identification procedure discussed in this paper depends upon several factors that include magnitude and distribution of noise terms, number of particles used, details of averaging of weights, number of global iterations, and details of zonation strategy (as has been used in Example 4.3). Establishing the nature of the estimators for the system parameters vis-à-vis these factors require further research. Moreover, the strategy of averaging of weights has enabled a reduction of number of calls to the FE software during the identification process. The basis for this strategy has remained intuitive in this study. Further studies to investigate the mathematical justification and alternative routes for minimizing the calls to FE software are needed. Finally we note that the various signal conditioning filters that are invariably used to eliminate high frequency electronic noise during data acquisition potentially could also eliminate genuine response components especially for nonlinear dynamical systems. A way forward here would be to introduce these filter equations into the state space model for the system under consideration. This aspect has not been investigated in the present study and requires further investigations.

Acknowledgements

This work has been supported by funding from Aeronautical Research and Development Board, Government of India and the Indian Railways (South-Western Division). The data in Section 4.3 has been obtained through a collective effort and CSM thanks his co-principal investigators in the project, Professors J.M. Chandra Kishen and Ananth Ramaswamy, for their contributions to this effort and for many useful discussions.

References

- [1] Juang JN. Applied system identification. NJ: Prentice Hall, PTR; 1994.
- [2] Ljung L. System identification: theory for the user. NJ: Prentice-Hall Inc.; 1997.
- [3] Maia NMM, Silva JMM, editors. Theoretical and experimental modal analysis. Baldock (UK): Research Studies Press; 1997. [Distributed by Wiley, Chichester].

- [4] Heylen W, Lammens S, Sas P. Modal analysis: theory and testing. Heverlee: Katholieke Universiteit Leuven; 1997.
- [5] Bendat JS. Nonlinear system techniques and applications. New York: Wiley; 1998.
- [6] Ewins DJ. Modal testing: theory, procedures and applications. Badlock: Research Studies Press; 2000.
- [7] Pintelon R, Schoukens J. System identification: a frequency domain approach. New York: IEEE Press; 2001.
- [8] Peeters B, Roeck GD. Stochastic system identification for operational modal analysis. ASME Journal of Dynamic Systems, Measurement, and Control 2001; 123:1–9.
- [9] Lieven NAL, Ewins DJ. Experimental modal analysis, theme issue. Philosophical Transactions of the Royal Society of London. Series A 2001;359:1–219.
- [10] Worden K, Tomlinson GP. Nonlinearity in structural dynamics: detection, identification and modeling. London: IOP Publishing; 2001.
- [11] Nelles O. Nonlinear system identification. Berlin (Heidelberg, NY): Springer-Verlag; 2001.
- [12] Kerschgen G, Worden K, Vakakis AF, Golinval JC. Past, present and future of nonlinear system identification in structural dynamics. Mechanical Systems and Signal Processing 2006;20(3):505–92.
- [13] Friswell MI, Mottershead JE. Finite element model updating in structural dynamics. Dordrecht: Kluwer Academic Publishers; 1996.
- [14] Doebling SW, Farrar CR, Prime MB. A summary review of vibration-based damage identification methods. The Shock and Vibration Digest 1998;30(2): 91–105.
- [15] Sohn H, Farrar CR, Hemez FM, Shunk DD, Stinemates DW, Nadler BR. A review of structural health monitoring literature: 1996–2001. USA: Los Alamos National Laboratory; 2003.
- [16] Ristic B, Arulampalam S, Gordon N. Beyond the Kalman filter: particle filters for tracking applications. Boston: Artech House; 2004.
- [17] Kalman RE. A new approach to linear filtering and prediction problems. Transactions of the ASME. Series D, Journal of Basic Engineering 1960;82: 35–45.
- [18] Kailath T. Lectures on Wiener and Kalman filtering. New York: Springer Verlag; 1981.
- [19] Brown RG, Hwang PYC. Introduction to random signals and applied Kalman filtering. 2nd ed. New York: John Wiley and Sons, Inc.; 1992.
- [20] Grewal MS, Andrews AP. Kalman filtering: theory and practice using Matlab. New York: John Wiley and Sons, Inc.; 2001.
- [21] Chui CK, Chen G. Kalman filtering with real time applications. New York: Springer; 1998.
- [22] Gordon NJ, Salmond DJ, Smith AFM. Novel approach to nonlinear/non-Gaussian Bayesian state estimation. IEE Proceedings F 1993;140(2): 107–13.
- [23] Tanizaki H. Nonlinear filters: estimation and applications. 2nd ed. Berlin: Springer Verlag; 1996.
- [24] Doucet A. On sequential simulation-based methods for Bayesian filtering. Technical report CUED/F-INFENG/TR.310 (1998). UK: Department of Engineering, University of Cambridge; 1998.
- [25] Liu JS, Chen R. Sequential Monte Carlo methods for dynamical systems. Journal of the American Statistical Association 1998;93:1032–44.
- [26] Pitt MK, Shephard N. Filtering via simulation: auxiliary particle filter. Journal of American Statistical Association 1999;94:59–599.
- [27] Doucet A, Godsill S, Andrieu C. On sequential Monte Carlo sampling methods for Bayesian filtering. Statistics and Computing 2000;10:197–208.
- [28] Iba Y. Population Monte Carlo algorithms. Transactions of the Japanese Society for Artificial Intelligence 2001;16(2):279–86.
- [29] Doucet A, de Freitas N, Gordon N. Sequential Monte Carlo methods in practice. New York: Springer; 2001.
- [30] Crisan D, Doucet A. A survey of convergence results on particle filtering methods for practitioners. IEEE Transactions on Signal Processing 2002;50(3): 736–46.
- [31] Cappé O, Godsill SJ, Moulines E. An overview of existing methods and recent advances in sequential Monte Carlo. Proceedings of the IEEE 2007;95(5): 899–924.
- [32] Doucet A, Johansen AM. A tutorial on particle filtering and smoothing: fifteen years later. 2008. http://www.cs.ubc.ca/~arnaud/doucet_johansen_tutorialPF.pdf [accessed 14.03.09].
- [33] Yun CB, Shinozuka M. Identification of nonlinear structural dynamic systems. Journal of Structural Mechanics 1980;8(2):187–203.
- [34] Hoshiya M, Saito E. Structural identification by extended Kalman filter. Journal of Engineering Mechanics, ASCE 1984;110(12):1757–70.
- [35] Imai H, Yun CB, Maruyama O, Shinozuka M. Fundamentals of system identification in structural dynamics. Probabilistic Engineering Mechanics 1989;4(4):162–73.
- [36] Corigliano A, Mariani S. Parameter identification in explicit structural dynamics: performance of the extended Kalman filter. Computer Methods in Applied Mechanics and Engineering 2004;193(36–38):3807–35.
- [37] Ghosh S, Roy D, Manohar CS. New forms of extended Kalman filter via transversal linearization and applications to structural system identification. Computer Methods in Applied Mechanics and Engineering 2007;196: 5063–83.
- [38] Ching J, Beck JL. Bayesian analysis of the phase II IASC–ASCE structural health monitoring experimental benchmark data. Journal of Engineering Mechanics, ASCE 2004;130(10):1233–44.
- [39] Manohar CS, Roy D. Monte Carlo filters for identification of nonlinear systems. Sadhana 2006;31(4):399–427.
- [40] Ching J, Beck JL, Porter KA. Bayesian state and parameter estimation of uncertain dynamical systems. Probabilistic Engineering Mechanics 2006; 21(1):81–96.
- [41] Ghosh S, Manohar CS, Roy D. Sequential importance sampling filters with a new proposal distribution for parameter identification of structural systems. Proceedings of the Royal Society of London. Series A 2008;464:25–47.
- [42] Sajeeb R, Manohar CS, Roy D. A conditionally linearized Monte Carlo filter in nonlinear structural dynamics. International Journal of Non-Linear Mechanics 2009;44(7):776–90.
- [43] Ghanem R, Shinozuka M. Structural system identification I: theory. Journal of Engineering Mechanics, ASCE 1995;121(2):255–64.
- [44] Shinozuka M, Ghanem R. Structural system identification II: experimental verification. Journal of Engineering Mechanics, ASCE 1995;121(2):265–73.
- [45] Namdeo V, Manohar CS. Nonlinear structural dynamical system identification using adaptive particle filters. Journal of Sound and Vibration 2007;306: 524–63.
- [46] Liu J, West M. Combined parameter and state estimation in simulation-based filtering. In: Doucet A, de Freitas N, Gordon N, editors. Sequential Monte Carlo methods in practice. New York: Springer; 2001. p. 197–223.
- [47] Storvik G. Particle filters for state–space models with the presence of unknown static parameters. IEEE Transactions on Signal Processing 2002;50(2):281–9.
- [48] Chopin N. A sequential particle filter method for static models. Biometrika 2002;89(3):539–51.
- [49] Doucet A, Tadic VB. Parameter estimation in general state–space models using particle methods. Annals of the Institute of Statistical Mathematics 2003; 55(2):409–22.
- [50] Ionides EL, Breto C, King AA. Inference for nonlinear dynamical systems. Proceedings of the National Academy of Sciences 2006;103(49):18438–43.
- [51] Tipireddy R, Nasrellah HA, Manohar CS. A Kalman filter based strategy for linear structural system identification based on multiple static and dynamic test data. Probabilistic Engineering Mechanics 2009;24:60–74.
- [52] Nasrellah HA, Manohar CS. Particle filters for structural system identification using multiple test and sensor data: a combined computational and experimental study. Structural Control and Health Monitoring 2009; doi:10.1002/stc.361.
- [53] Smith AFM, Gelfand AE. Bayesian statistics without tears: a sampling–resampling perspective. American Statistics 1992;46(2):84–8.
- [54] Radhika B, Manohar CS. Reliability models for existing structures based on dynamic state estimation and data based asymptotic extreme value analysis. Probabilistic Engineering Mechanics 2010;25:393–405.
- [55] Bates SJ, Siens J, Langley DS. Formulation of the Audze–Eglais uniform Latin hypercube design of experiments. Advances in Engineering Software 2003; 34(8):493–506.
- [56] Bathe KJ, Ramm E, Wilson EL. Finite element formulations for large deformation dynamic analysis. International Journal for Numerical Methods in Engineering 1975;9:353–86.
- [57] NISA. NISA II verification manual, version 16.1. Troy: Cranes Software Inc.; 2009.